


## Research Article

# Study on Properties of Magnesium Oxychloride Cement Solidified Soil

Haoyu Wang,<sup>1</sup> Jinbao Zhang,<sup>2</sup> Xiaohui Yan,<sup>1</sup> and Rui Xiong<sup>1</sup> 

<sup>1</sup>School of Materials Science and Engineering, Chang'an University, Xi'an 710061, China

<sup>2</sup>Qinghai Transportation Holding Group Co., Ltd., Xining 810001, China

Correspondence should be addressed to Rui Xiong; xiongrui@chd.edu.cn

Received 19 March 2022; Revised 8 May 2022; Accepted 30 August 2022; Published 12 September 2022

Academic Editor: Baskaran Rangasamy

Copyright © 2022 Haoyu Wang et al. This is an open access article distributed under the Creative Commons Attribution License, which permits unrestricted use, distribution, and reproduction in any medium, provided the original work is properly cited.

Due to the poor performance of ordinary Portland cement (OPC) as a solidified soil road and the large pollution in the production process, environment-friendly magnesium oxychloride cement (MOC) was used as the soil curing agent to prepare the solidified soil, exploring the optimal ratio of various raw materials when MOC is used as a curing agent. Analyzing the properties of MOC solidified soil in the application of road subgrade. This paper tests compaction, mechanical properties, and durability of the MOC solidified soil, simulates the development trend of 7 days unconfined compressive strength of MOC solidified soil, and then analyzes the hydration process and strengthens the formation mechanism of MOC in solidified soil. The study found that the addition of MOC as a curing agent to the soil can effectively improve the compaction and mechanical properties of the soil. Matlab simulation found that when the MgO content is 5.5% to 6% and the ratio of raw materials MgO, MgCl<sub>2</sub>, and H<sub>2</sub>O is 2.45 : 1 : 14 to 6.3 : 1 : 14, the performance of MOC solidified soil is excellent. Fitting UCS data, it is found that MOC solidified soil has early strength characteristics. The excellent compaction and mechanical properties of MOC solidified soil are due to the formation of a small amount of phase 5 and layered Mg(OH)<sub>2</sub> by the hydration of MOC, and the formation of amorphous gel with SiO<sub>2</sub> in the soil. This reaction improves soil compaction and reduces internal porosity from a microscopic perspective. The strength loss rate of MOC solidified soil is higher after immersion in water at the initial stage of curing, but it is still better than that of traditional cement-based solidified soil. Poor performance after immersion in water is associated with disruption of the network-like structure. As an environment-friendly soil curing agent, MOC can be used in engineering practice with low environmental humidity.

## 1. Introduction

Soft soil can lead to potential safety hazards caused by poor bearing capacity during construction; high soil expansion will generate subgrade shrinkage, resulting in pavement cracking and reduced service life [1–3]. Soil stabilization is one of the soil improvement methods in geotechnical engineering. In addition, cement and lime stabilizations are two of the most commonly used methods in recent years [4, 5]. The addition of traditional curing agents such as ordinary Portland cement (OPC) and lime can improve soil mechanical properties and durability [6–8]. Further, the study found that after adding MgO to the OPC stabilized soil, the pH of the soil increased with the increase of

magnesium slag. During the hydration process, calcium aluminate hydrate (C-A-H) and calcium silicate hydrate gel (C-S-H) were produced, which improved soil conditions [9, 10]. However, traditional OPC curing agents have problems such as limited mechanical strength, poor durability, poor volume stability, high pollution in the production process, and high CO<sub>2</sub> emissions [11–14].

Magnesium oxychloride cement (MOC) is an environment-friendly magnesia cementitious material prepared by lightly burning magnesium oxide, magnesium chloride and water [15]. Due to its fast-setting speed, high mechanical strength, good wear resistance, salt resistance and halogen corrosion, simple production process, and low cost, it is widely used in construction materials, biological materials,

TABLE 1: Technical indexes of fine-grained soil.

Nominal maximum particle size (mm)	Maximum particle size (mm)	Moisture content (%)	Liquid limit (%)	Plastic limit (%)	Plasticity index
2.36	4.75	8.7	23.8	14.7	9.1

TABLE 2: Physical properties and chemical composition of raw materials.

Raw materials	Chemical composition (%)				
	MgO	SiO <sub>2</sub>	Al <sub>2</sub> O <sub>3</sub>	CaO	Fe <sub>2</sub> O <sub>3</sub>
Light burned magnesite	80.21	6.87	2.01	1.58	1.32
Industrial magnesium chloride	85.43	6.65	1.82	1.33	1.31

and other fields [16–18]. The salt lakes in the Qinghai area of China have sufficient reserves of magnesium salts and high grades [19]. Part of the waste MOC can be reused after recycling and processing, such as superhydrophobic magnesium oxychloride cement [20]. Waste building materials and industrial residues can also be used to prepare MOC or improve the performance of MOC, such as waste gypsum, ammonia alkali residue, and fly ash [21–23]. Studies have shown that when MOC is used as a soil stabilizer, it can form an amorphous gel product covering the surface of soil particles, effectively cementing soil particles and filling inter-particle voids. It also greatly improves soil mechanical properties and reduces harmful ion leakage. The optimum dosage of MOC as a soil stabilizer is 10% [24–26]. At present, the environment-friendly soil stabilizer MOC has not attracted enough attention, and there are few related researches and experiments. The optimal raw material ratio and maintenance method of MOC as a soil stabilizer still need to be studied. Various properties of soil after curing with MOC have yet to be tested, and the microscopic mechanism remains to be explored.

This paper analyzes and simulates the optimal raw material ratio of MOC as a curing agent through a macro compaction test, mechanical test, durability test, and MATLAB software. Scanning electron microscope (SEM) and X-ray diffractometer (XRD) are used to observe the microstructure of MOC solidified soil. The microscopic mechanism of MOC reinforced fine-grained soil has been explored. It is hoped that this study can provide a valuable reference for the subsequent use of MOCs as soil stabilizers.

## 2. Materials and Methods

**2.1. Materials.** The test soil was fine-grained soil with a plasticity index of 9.1, which has low liquid limit clay. Technical indexes are shown in Table 1. The raw materials for the preparation of MOC were lightly burned magnesite and industrial magnesium chloride. MgO was a light-burned magnesite powder produced in Haicheng, Liaoning Province. The content of MgO was more than 85%, and the content of active MgO was 60%. The specific surface area of the light-burned magnesite powder was 340 m<sup>2</sup>/kg. The physical properties and chemical composition are shown in Table 2. The particle size distribution of MgO is shown in

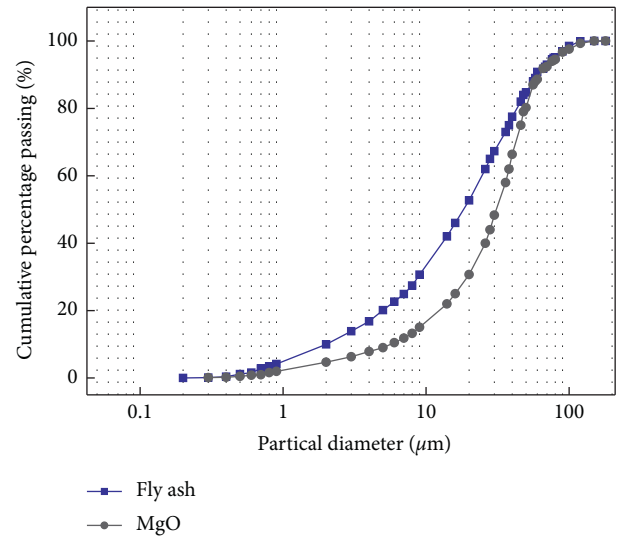


FIGURE 1: Particle size distribution of MgO.

Figure 1. MgCl<sub>2</sub> was produced by Qinghai Golmud. The content of magnesium chloride was more than 45%.

**2.2. Experimental Methods.** Mechanical properties and durability tests were used to evaluate the performance of MOC stabilized soil. Test flow is shown in Figure 2. The following is a detailed description of the mechanical properties and durability tests.

**2.2.1. Compaction Test.** The compaction test (Method A) was adopted JTG-E51-2009. The size of the tube used in the test was 10.0 cm × 12.7 cm (inner diameter × height) and the volume was 997 cm<sup>3</sup>. Five different water contents were set, with a difference of 2.0% in sequence. The ratio of the compaction test is shown in Table 3.

**2.2.2. Mechanical Property Analysis.** The differences in mechanical properties of OPC and MOC solidified soils were compared. OPC consisted of 5% 42.5 cement and 11% water content. The effects of different ratios of raw materials on the mechanical strength of MOC solidified soil were discussed. The MOC raw material ratio is shown in Table 4. The

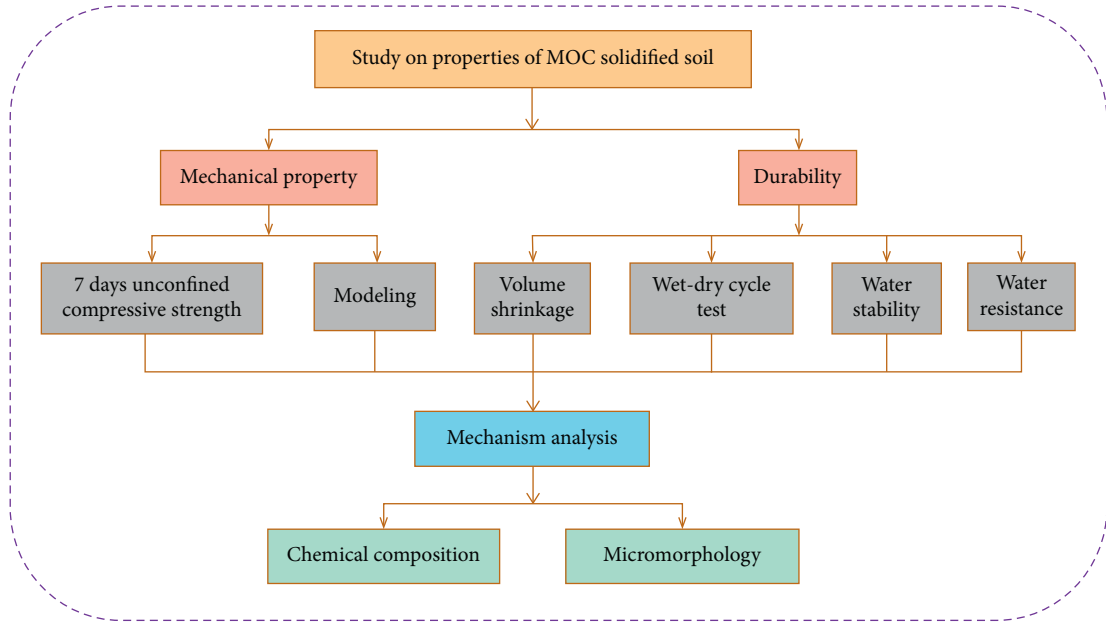


FIGURE 2: Test flow chart.

TABLE 3: Compaction test ratios.

Number	MgO (%)	MgCl <sub>2</sub> :H <sub>2</sub> O	Water content
1	3	1:15	7%, 9%, 11%, 13%, 15%
2	4	1:15	7%, 9%, 11%, 13%, 15%
3	5	1:15	7%, 9%, 11%, 13%, 15%
4	4	1:10	7%, 9%, 11%, 13%, 15%
5	4	1:15	7%, 9%, 11%, 13%, 15%
6	4	1:20	7%, 9%, 11%, 13%, 15%

TABLE 4: MOC raw material ratios.

Number	MgO (%)	MgCl <sub>2</sub> :H <sub>2</sub> O	MgO:MgCl <sub>2</sub> :H <sub>2</sub> O	Moisture content (%)
A1	3	1:10	1.42:1:10	9.5
A2	3	1:15	2.13:1:15	9.5
A3	3	1:20	2.84:1:20	9.5
B1	4	1:10	1.80:1:10	10
B2	4	1:15	2.70:1:15	10
B3	4	1:20	3.60:1:20	10
C1	5	1:10	2.14:1:10	10.5
C2	5	1:15	3.21:1:15	10.5
C3	5	1:20	4.29:1:20	10.5
D1	6	1:10	2.45:1:10	11
D2	6	1:15	3.68:1:15	11
D3	6	1:20	4.91:1:20	11
E1	7	1:10	2.63:1:10	12
E2	7	1:15	3.94:1:15	12
E3	7	1:20	4.25:1:20	12

specimens were prepared and cured in an indoor environment for 7 days, and the unconfined compressive strength (UCS) was tested. The variation trend of 7 days UCS of MOC solidified soil was simulated by MATLAB.

**2.2.3. Durability Analysis.** The durability of MOC solidified soil was evaluated by volume shrinkage test, wet-dry cycle test, water stability test, and infiltration conductivity test. The specimen size was  $\Phi 50 \times 50$  mm cylindrical specimens.



FIGURE 3: Digital conductivity meter.

The volume shrinkage test adopted the ratio of B2, C2, and D2, and the curing temperature was  $20 \pm 2^\circ\text{C}$ . The original height and diameter of specimens were measured with a vernier caliper, then continued to test the data for 1 to 7 days of curing, and calculated the volume change.

The wet-dry cycle test was prepared according to the C2 ratio, the static pressure method was compacted and the demoulding curing was carried out for 7 days. The number of wet-dry cycles was set to 0, 1, 3, and 5 times.

The water stability test applied C2 ratio and the specimen standard curing for 48 h in  $20 \pm 2^\circ\text{C}$ . After the specimen had been formed, the UCS was measured after immersing in water for 24 h on the third and seventh day, respectively. Water stability coefficient of the specimens was calculated according to

$$\text{water stability coefficient} = \frac{\text{UCS of immersing water 24h}}{\text{UCS of standard care}}. \quad (1)$$

The ratio of B2, C2, and D2 were set for the water resistance test, and the curing temperature was  $20 \pm 2^\circ\text{C}$ . After curing for 7 days, the specimens were completely immersed in water, and the amount of water in each group was strictly controlled to be exactly the same. After immersing for 6 h, the conductivity changes of water were measured. The instrument used is a DDS-11A digital conductivity meter as shown in Figure 3.

**2.2.4. Micro Tests.** Scanning electron microscope was used to observe the microscopic morphology of MOC solidified soil, and X-ray diffractometer was used to test the chemical composition of MOC solidified soil. The sample design scheme of the microscopic analysis test is shown in Table 5.

### 3. Results and Discussion

**3.1. MOC Solidified Soil Compaction.** Figure 4 shows the effect of different raw material ratios on the maximum dry density of MOC solidified soil. The maximum dry density can reflect the compaction of MOC solidified soil well. As shown in Figure 4, the change of MgO content has a great influence on the maximum dry density of MOC solidified soil. In Figure 4(a), when the content of MgO is 5%, the maximum dry density reaches  $2.008 \text{ g/cm}^3$  compared with 3% MgO, which is increased by 15.33%. The curing effect improved continuously with the increase of MgO content. In Figure 4(b), the curing effect has little correlation with the ratio of  $\text{MgCl}_2$  to  $\text{H}_2\text{O}$ .

**3.2. Mechanical Properties of MOC Solidified Soil.** Figure 5 illustrates 7 days UCS of MOC solidified soil specimens with different ratios. The strength of C2, D1, D2, E1, and E2 samples are higher than OPC solidified soil. The strength of D2 reaches 1.76 MPa, which is composed of 6% MgO and the ratio of  $\text{MgCl}_2$  to  $\text{H}_2\text{O}$  is 1:15. Compared with OPC solidified soil, D2 is increased by 30.4%. Compared with traditional cement-based soil stabilizers [27, 28], such as OPC and calcium sulfoaluminate cement (CSA), 7 days UCS value of MOC stabilized soil is the highest. Therefore, in order to make the strength of the MOC solidified soil higher, MgO should not be less than 5% and the ratio of  $\text{MgCl}_2$  to  $\text{H}_2\text{O}$  is about 1 to 10~15.

In order to explore the effect of the raw material ratio on the 7 days UCS of MOC solidified soil, MATLAB was used to fit the ratio of MgO,  $\text{MgCl}_2$ , and  $\text{H}_2\text{O}$  on the surface. Three fitting surfaces are shown in Figure 6. The  $x$ -axis is the content of MgO (a%). The  $y$ -axis is the molar ratio of  $\text{MgCl}_2$  to  $\text{H}_2\text{O}$  (1:b), and  $z$ -axis is the 7 days UCS.

The functional equations obtained by the fitting of Models I, II, and III are sequentially shown in

$$\sigma_1 = -1.876 + 43.87x + 0.293y - 252.4x^2 - 0.009y^2 - 0.58xy, \quad (2)$$

$$\sigma_2 = 5.03 - 239.6x - 0.253y + 3955x^2 + 0.008y^2 + 11.03xy - 2.72ex^2 - 5.714x^2y - 0.368xy^2, \quad (3)$$

$$\sigma_3 = -1.45 + 19.17x + 0.312y - 0.58xy - 0.1y^2. \quad (4)$$

The statistical parameter lists of the three models were compared, as shown in Table 6. Statistical parameters include error term degrees of freedom ( $f$ ), error sum of squares (SSE), root mean square (RMSE), coefficient of determination  $R$ -square, and adjusted  $R$ -square.

The SSE and RMSE of Model II tend to be closer to 0 and the  $R$ -square is closer to 1. It can be seen that the fitting degree of Model II for MOC solidified soil is better. In addition, from the models in Figure 6 and Table 6, it can be seen that Model II is matched only when the MgO content is greater than 5%, and the fitting degree of the data is better under the same condition. When the MgO content is lower, the strength predicted in Model II increases, but the actual strength decreases. Model II is the opposite of the actual situation, so it is not adopted. Taking into account comprehensively, Model I is suitable for characterizing the 7 days UCS of MOC solidified soil with different proportions.

The shaded part of Figure 7(b) indicates that 7 days UCS of MOC solidified soil is higher than that of OPC solidified soil. It can be seen from Figure 7 that the optimum content of MgO is 5.5%~6% and the ratio of  $\text{MgCl}_2$  to  $\text{H}_2\text{O}$  is 1:14. At this dosage range, the strength reaches more than 1.6 MPa, and the effect of constantly increasing the dosage of MgO on improving the strength is not significant. Combined with the experimental data, 7 days UCS of C2, D1, D2, E1, and E2 are better than that of OPC solidified soil, and the strength of D2 reaches 1.76 MPa, which is 30.4% higher than that of OPC solidified soil. 7 days UCS of MOC solidified soil is more

TABLE 5: Microscopic test sample design scheme.

Number	MgO (%)	MgCl <sub>2</sub> : H <sub>2</sub> O	Maintenance method
1	5	1:15	Standard curing 7 d
2	5	1:15	Standard curing for 7 d, last day soaked in water
3	6	1:10	Standard curing 7 d
4	5	1:15	Standard curing 6 h

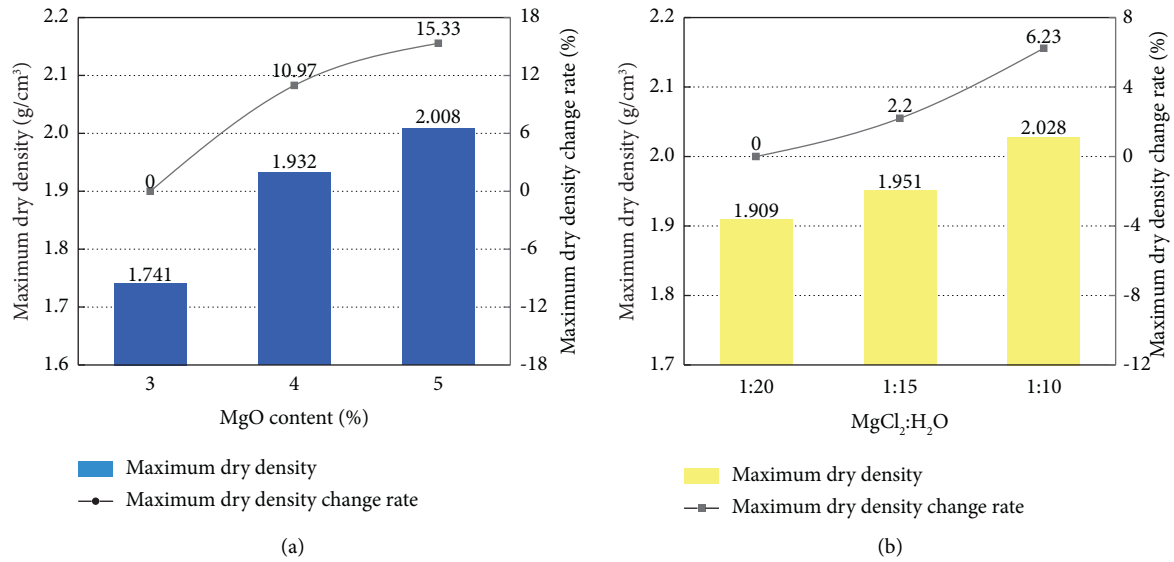
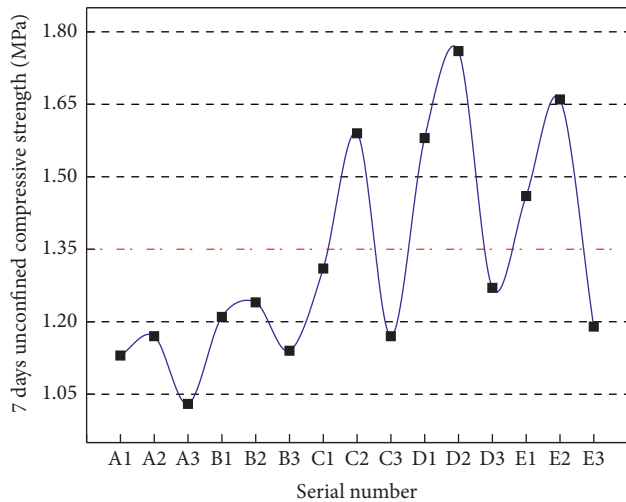
FIGURE 4: Influence of raw material ratio on the maximum dry density of MOC solidified soil. (a) Different MgO contents. (b) Different ratios of MgCl<sub>2</sub> to H<sub>2</sub>O.

FIGURE 5: Unconfined compressive strength of specimen for 7 days.

than 1.0 MPa. Combining with Table 7, it can be seen that it meets the requirements of the sub-base of secondary and lower highways under medium and light traffic loads.

In order to study the effect of curing age on UCS of MOC solidified soil, different curing times were taken and UCS tests were carried out. Figure 8 shows the UCS change rate of specimens after different curing aging. UCS development trends of MOC solidified soil and OPC solidified soil are shown in Figure 9.

Figures 8 and 9 demonstrate that the UCS of MOC solidified soil develops faster than that of OPC solidified soil. 3 days strength reaches 90% of 7 days strength and the 28 days strength is significantly higher than that of the OPC solidified soil. It shows that MOC added to fine-grained soil as a curing agent can effectively improve the mechanical properties of the solidified soil.

**3.3. Durability of MOC Solidified Soil.** Figure 10 represents the volume shrinkage of MOC solidified soil as the ratio change of MgCl<sub>2</sub> and H<sub>2</sub>O. After the MOC solidified soil was formed, a slight volume expansion occurred on the first day, then a certain degree of shrinkage came up. When MgO content is 4%, 7 days change rate is 2.3%. When MgO content is 6%, the change rate is 1.27%. Overall, the volume change rate of MOC solidified soil was slight.

Under the natural environment, the early soil is easy to absorb water and swell. With the extension of time, the water in the soil gradually volatilizes and shrinks in volume, which is easy to produce a large volume change rate. Nevertheless, MOC can play a role in consolidating and MgO has a certain expansion, which offsets part of the soil autogenous shrinkage and reduces the volume change rate of MOC solidified soil.

After the wet-dry cycle test, the strength loss rate and volume shrinkage rate of MOC solidified soil (C2) are shown in Figure 11. Wet-dry cycles have little effect on the volume shrinkage of MOC solidified soil, but have a greater effect on

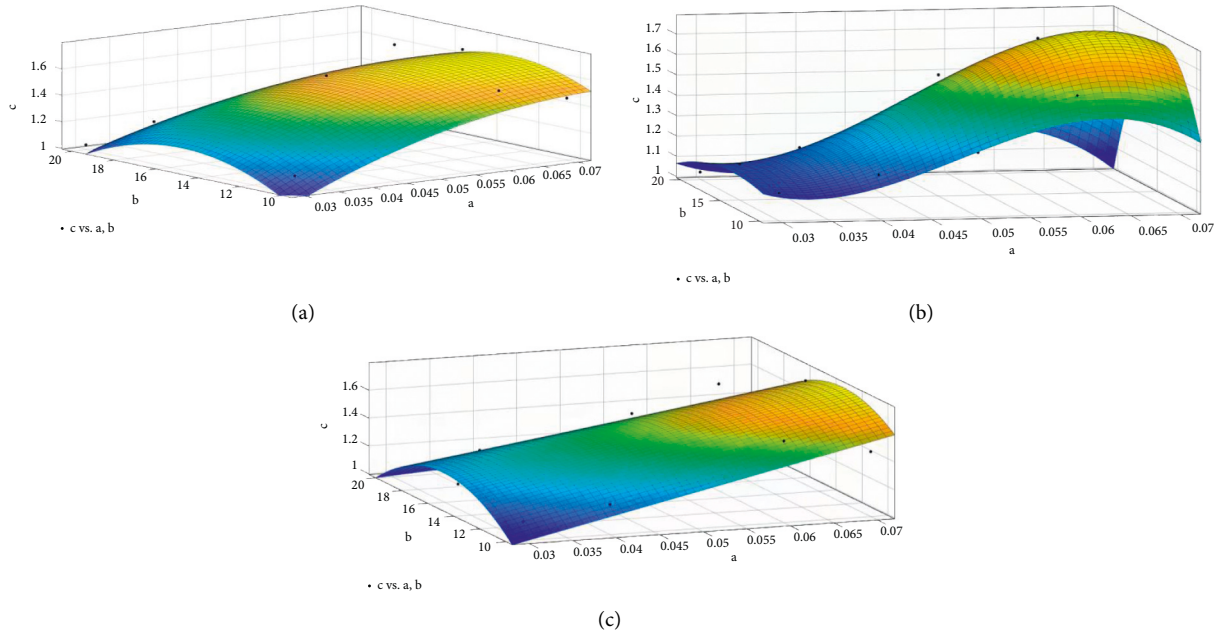


FIGURE 6: Three fitting surfaces. (a) Fitting surface of model I. (b) Fitting surface of model II. (c) Fitting surface of model III.

TABLE 6: Statistical parameters of different models.

Models	$f$	SSE	RMSE	$R$ -square	Adjusted $R$ -square
I	9	0.1093	0.1102	0.8568	0.7772
II	6	0.0207	0.0587	0.9729	0.9369
III	10	0.1286	0.1134	0.8315	0.7641

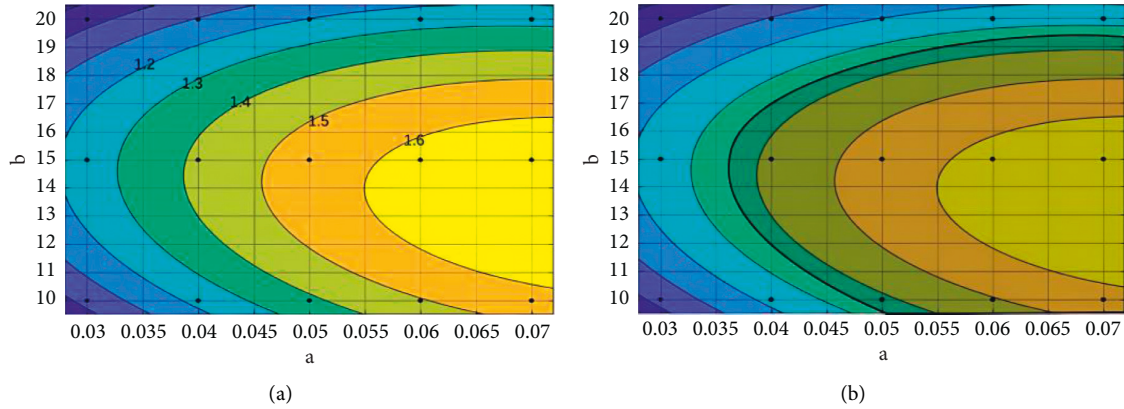


FIGURE 7: 7 days UCS contour map of MOC and OPC solidified soils. (a) Contour map of MOC solidified soil. (b) Comparison of MOC and OPC solidified soil contour map.

UCS. After 5 cycles, the volume change rate of MOC solidified soil is only 1.98%, and the strength loss rate is as high as 41.92%. By simply fitting the data, it can be seen that the strength loss rate decreases significantly before the 6th time, and becomes flat at the 9th time. The volume shrinkage rate of C2 fluctuates sharply only before 3 times, and fluctuates in a small range since then.

Figure 12 shows the strength change rate of the MOC solidified soil specimens before and after immersion in

water. After curing for 48 hours, improving with the age, the UCS of the immersed specimens decreased by 80.4% and 36.5% compared with the unimmersed specimens. After immersion in water for 24 h on the seventh day, the strength of the CSA solidified soil was only 0.6 MPa [27]. The strength of the MOC solidified soil is still as high as 1.26 MPa.

To sum up, MOC solidified soil has poor water stability and is sensitive to moisture and environmental humidity. With the increase of age, the strength loss rate of the

TABLE 7: Chinese cement-based material 7 days UCS standard (MPa).

Structural layer	Highway grade	Extremely heavy traffic	Heavy traffic	Medium and light heavy traffic
Subbase	Class 1 and above highways	3.0~5.0	2.5~4.5	2.0~4.0
	Secondary and lower highways	2.5~4.5	2.0~4.0	1.0~3.0

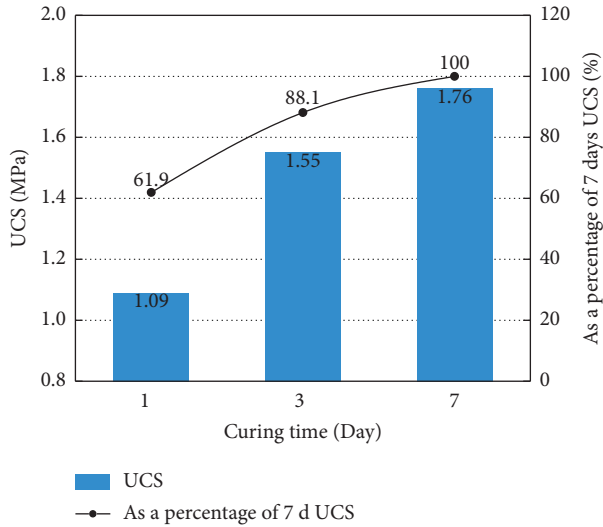


FIGURE 8: UCS of MOC solidified soil with different curing time.

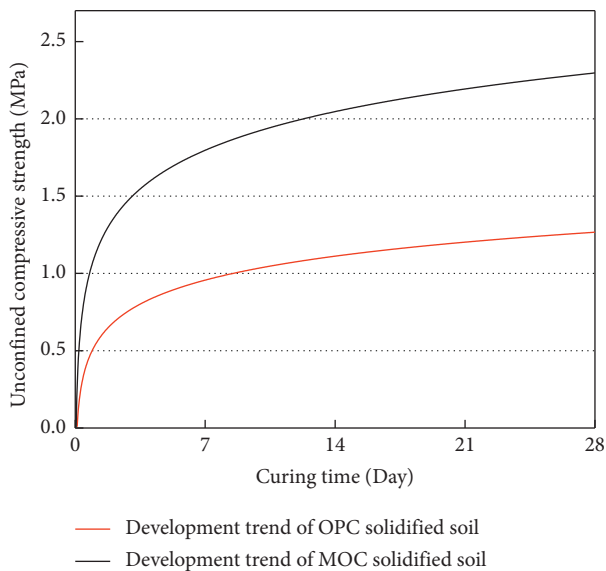


FIGURE 9: Strength prediction curve of OPC and MOC solidified soil.

specimens after immersing in water gradually decreases. In particular, during the initial maintenance, contacting with water should be avoided or the ambient humidity should be reduced. However, compared with other cement-based solidified soils, it still has better water resistance.

As illustrated in Figure 13, the electrical conductivity of the samples with different ratios in the infiltration solution is compared. As the ratio of  $\text{MgCl}_2$  to  $\text{H}_2\text{O}$  increases, the electrical conductivity gradually

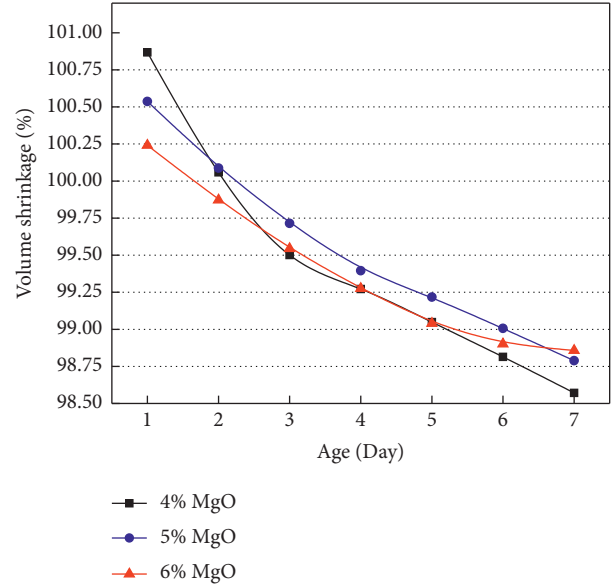


FIGURE 10: Volume shrinkage rate of MOC solidified soil with different ratios.

decreases, and it enhances continuity with the increase of  $\text{MgO}$  content. The change of conductivity is more correlated with the ratio of  $\text{MgCl}_2$  to  $\text{H}_2\text{O}$ , and the effect of  $\text{MgO}$  content is less. When the MOC solidified soil was soaked in water, free  $\text{Cl}^-$  ions played a conductive role, and  $\text{Mg}^{2+}$  ions might be transformed into  $\text{Mg}(\text{OH})_2$  and  $\text{MgCO}_3$ .

Because MOC is an unsaturated porous, multiphase material, its main strength phase (phase 5) is an unstable crystalline phase, which is prone to hydrolysis in water environment. After immersing in water, the needle-like dense structure was transformed into a loosely structured  $\text{Mg}(\text{OH})_2$ . Therefore, the density of MOC decreases and the internal voids increase, which led to poor water resistance and mechanical properties.

**3.4. Microstructure.** The XRD patterns of the four samples are shown in Figure 14. Sample 1 contained more phase 5, a small amount of  $\text{MgO}$  and  $\text{SiO}_2$  phases. It indicated that the reaction of active  $\text{MgO}$  was relatively complete, and it reacted with  $\text{SiO}_2$  in the soil to form an amorphous gelling substance. Calcium was derived from fine-grained soils and impurities in raw materials.

After sample 2 absorbed water, the  $\text{Mg}^{2+}$  concentration in the system decreased. This phenomenon led to the instability of the presence of alkaline hydrates on the surface, and phase 5 hydrolysis reaction occurred to generate  $\text{Mg}(\text{OH})_2$ . In addition, free  $\text{Mg}^{2+}$  was carbonized to form  $\text{MgCO}_3$  and  $\text{MgCO}_3 \cdot \text{ClOH} \cdot 2\text{H}_2\text{O}$ .  $\text{MgCO}_3 \cdot \text{ClOH} \cdot 2\text{H}_2\text{O}$  was

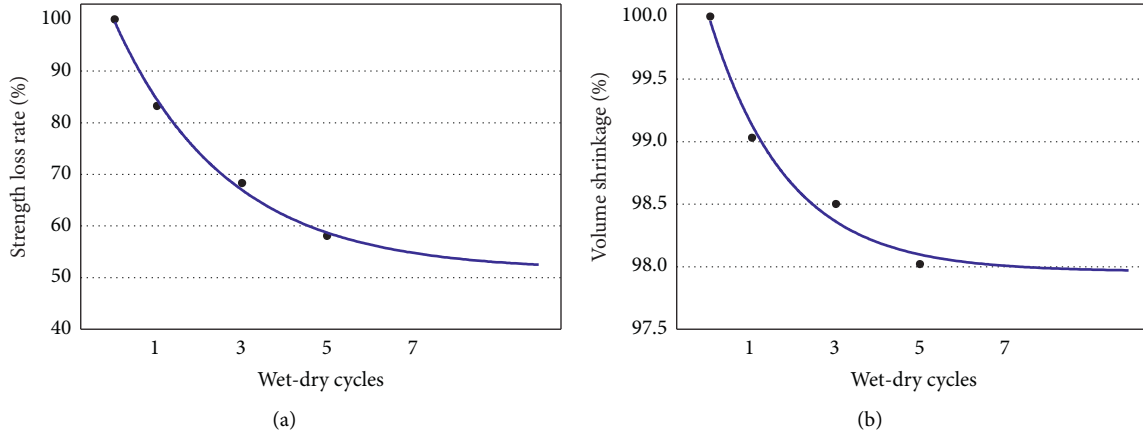


FIGURE 11: Effects of different wet-dry cycles on strength and volume. (a) Strength loss rate. (b) Volume shrinkage.

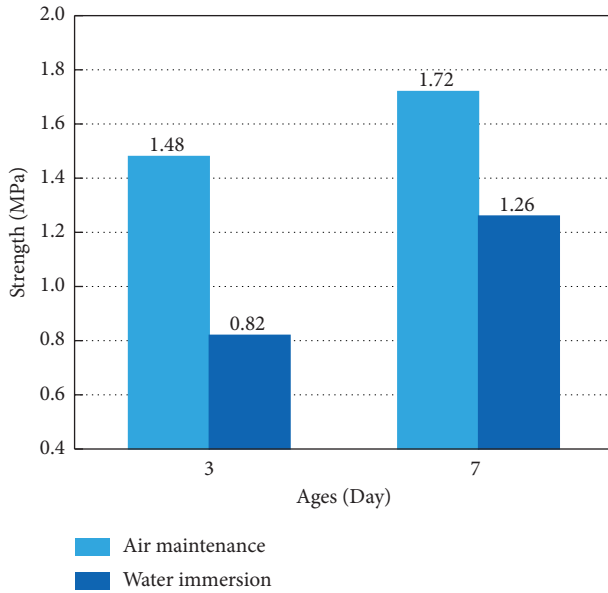


FIGURE 12: Changes in strength of MOC solidified soil after water immersion.

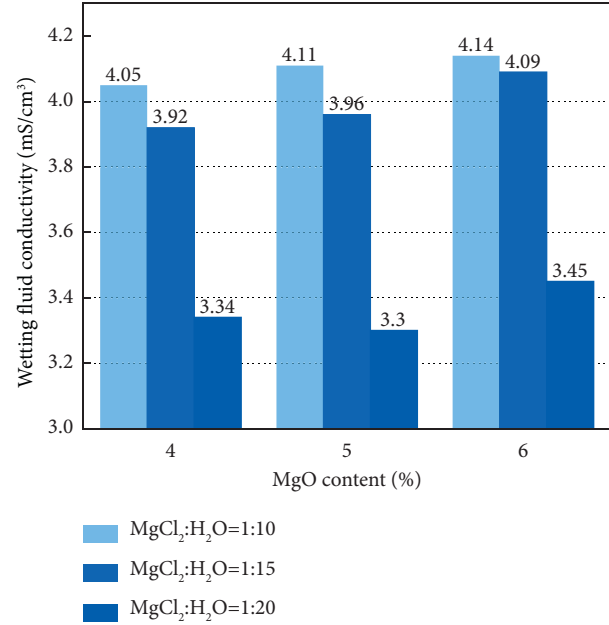
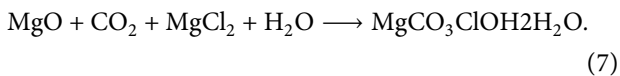
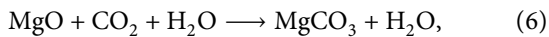
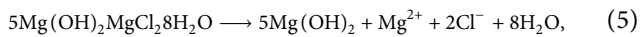


FIGURE 13: Infiltration conductivity of MOC solidified soil with different proportions.

not stable, and would continue to react in the solidified soil under the condition of sufficient water to generate  $\text{Mg}(\text{ClO}_2)_2 \cdot (\text{H}_2\text{O})_6$  [29]. The hydrolysis reaction is indicated in formula (5), and the carbonization reaction is presented in



The spectrum of sample 3 was similar to that of sample 1. Sample 3 has a higher content of phase 5 and less  $\text{SiO}_2$ . It showed that the curing reaction of sample 3 was more complete. The  $\text{SiO}_2$  content of sample 4 was very high, and

phase 5 began to appear. A small amount of MgO could still be seen in the sample. It illustrated that the curing reaction was still continuing when curing under standard conditions for 6 h.

Figure 15 indicates the SEM of the four samples. In sample 1, it can be observed that the surface of soil particles is covered with a large number of amorphous gelling products, lamellar  $\text{Mg}(\text{OH})_2$ , and a few needle-like phase 5. The gelling product and the lamellar  $\text{Mg}(\text{OH})_2$  are closely connected, and a small amount of phase 5 fills the voids in the soil to form a network structure and improve the compaction and mechanical properties of the soil.

Sample 2 was soaked in water after the hydration product was formed. On the one hand, phase 5 hydrolysis reaction occurred to produce loosely packed triangular pyramid  $\text{Mg}(\text{OH})_2$ , which distributed along the soil voids.

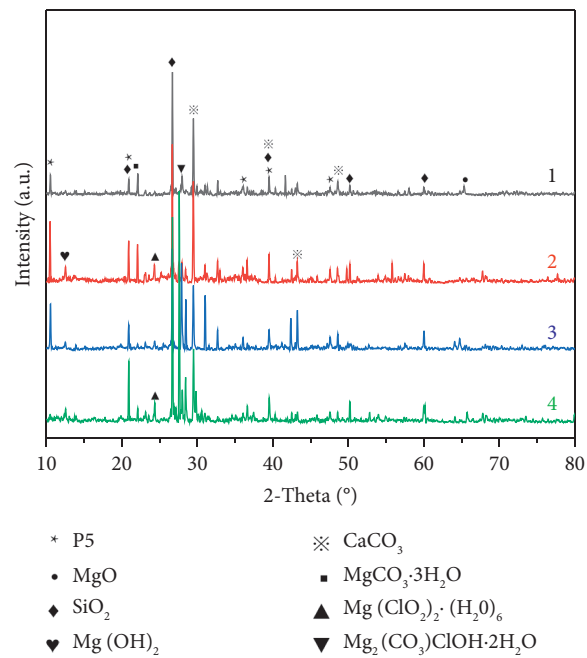


FIGURE 14: XRD analysis.

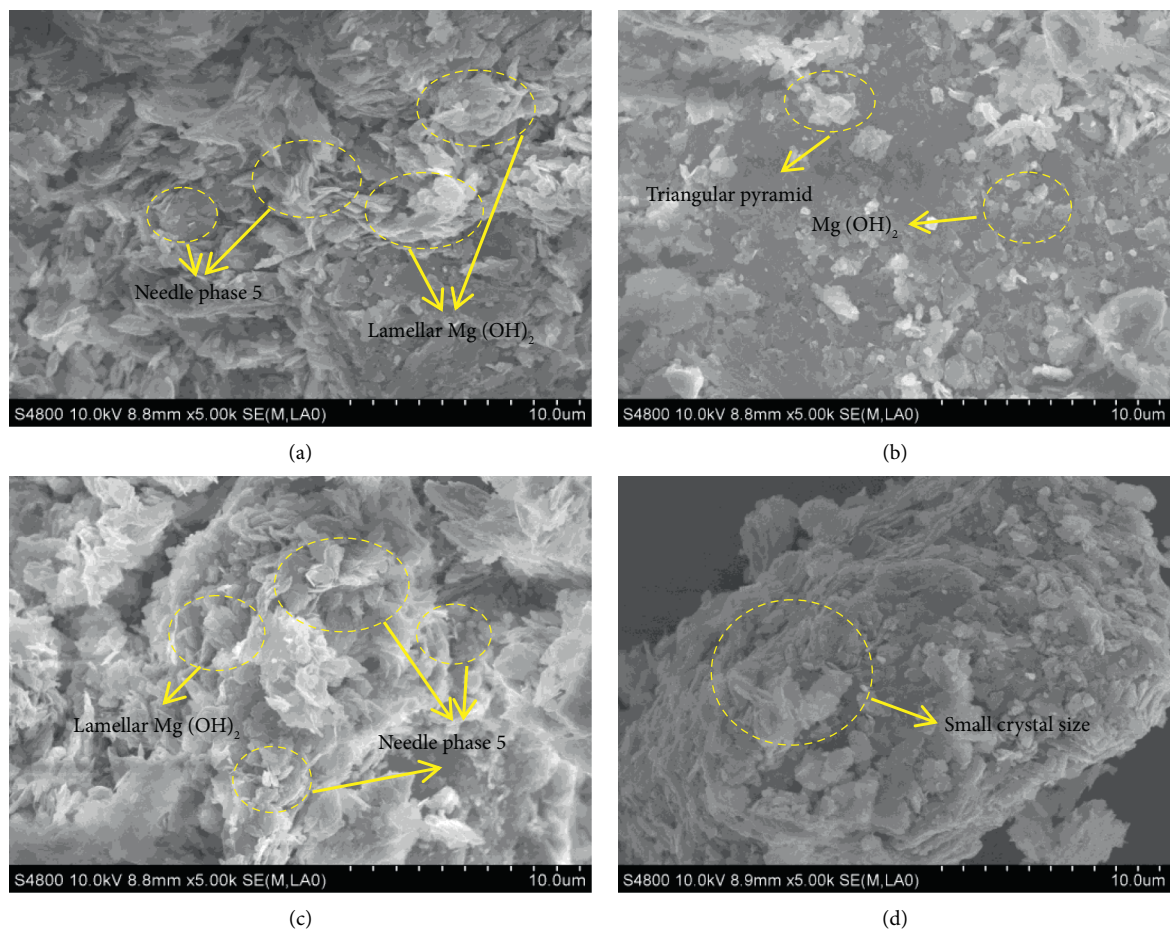


FIGURE 15: SEM analysis. (a) Sample 1, (b) Sample 2. (c) Sample 3, and (d) Sample 4.

And part of  $\text{Mg}(\text{OH})_2$  reacted with  $\text{CO}_2$  dissolved in water to form  $\text{MgCO}_3$ , attaching to the unhydrolyzed hydration product in the form of massive grains. On the other hand, the soil expands after the flood, causing the network structure to be destroyed. Therefore, larger voids could be seen, and the density of MOC solidified soil decreased.

After increasing the active  $\text{MgO}$  content and the ratio of  $\text{MgCl}_2$ , the amorphous gel, lamellar  $\text{Mg}(\text{OH})_2$ , and needle-like phase 5 were superimposed on each other to form a network structure, and soil particles could hardly be seen. The reaction greatly increases soil density, it is consistent with the above compaction degree and mechanical property analysis.

For sample 4 had smaller size amorphous gels as well as layered  $\text{Mg}(\text{OH})_2$ . Because of the short curing time, the activated magnesium oxide had not fully reacted, the strength mainly depended on the consolidation of soil particles by the gel tissue produced by the previous hydration. At the same time, it also reflects that a small amount of the phase 5 appeared in MOC solidified soil at the beginning of curing for 6 h, which is consistent with the fast-setting characteristics of MOC.

Through the above microscopic experiments, it can be concluded that the process of using MOC as a curing agent to solidified soil includes: active  $\text{MgO}$ ,  $\text{H}_2\text{O}$ , and silicon in soil form M-S-H gel, which is wrapped on the surface of soil; then  $\text{Cl}^-$  in dissolved  $\text{MgCl}_2$  reacted with the gel layer to form the main strength phase (phase 5). Phase 5 continued to grow to fill the gaps between soil particles and cross-linked to form a network structure to consolidate the soil particles. The reason for the poor performance of MOC solidified soil after immersing is that the phase 5 was hydrolyzed to form layered  $\text{Mg}(\text{OH})_2$ , and part of the  $\text{Mg}(\text{OH})_2$  was carbonized to form  $\text{MgCO}_3$ , which destroys the network structure formed by the phase 5 and soil particles.

#### 4. Conclusions

In this paper, MOC stabilized soil was studied through laboratory experiments and mathematical modeling, and the feasibility of MOC as an environmentally friendly soil-stabilizing agent was described and discussed. Through a series of mechanical properties, durability and microstructure test, engineering properties, main hydration products and microstructure characteristics of MOC stabilized soil were explored, and the optimal raw material ratio of MOC as a soil curing agent was proposed. The precautions and application fields of MOC as a soil stabilizer in engineering practice are given. According to the experimental data and model, the following conclusions are drawn:

- (1) Compared with existing cement-based soil stabilizers, such as OPC and CSA, the MOC curing agent can effectively improve soil compaction and mechanical properties. Combined with the specification requirements under the action of different grades of highways and traffic loads, MOC solidified soil is

suitable for the sub-base of secondary and lower highways under light traffic load.

- (2) In-depth research was carried out on the strength development law of MOC solidified soil with different ratios of raw materials. The test found that when the content of  $\text{MgO}$  is 6% and the ratio of  $\text{MgO}$ ,  $\text{MgCl}_2$ , and  $\text{H}_2\text{O}$  is 3.68:1:15, the properties of MOC solidified soil are the best. Then the relevant mathematical model was established according to the test data, and the optimal ratio of raw materials was obtained as  $\text{MgO}$  content in 5.5%~6% and the ratio of  $\text{MgCl}_2$  to  $\text{H}_2\text{O}$  is 1:14. After the test data was fitted to analyze the strength change trend, it was found that the MOC solidified soil had the characteristics of early strength, and the construction time should be controlled in practice.
- (3) The strength loss rate of MOC solidified soil after water immersion in the initial stage of curing is higher, but it is still better than that of traditional cement-based solidified soil. MOC solidified soil should be avoided in coastal areas, areas with sufficient rainfall, and the sub-base of permeable pavement. Water erosion should be minimized in the initial stage of maintenance.
- (4) According to mechanical test and durability test combined with microscopic morphology, the hydration process of MOC in soil was analyzed, and the strength formation mechanism of MOC that used as a soil stabilizer was explained:  $\text{MgO}$ ,  $\text{H}_2\text{O}$ , and  $\text{SiO}_2$  formed M-S-H gel to wrap soil particles. It further reacts with  $\text{MgCl}_2$  to form the main strength phase (phase 5) and lamellar  $\text{Mg}(\text{OH})_2$ , and the soil particles form a cross-linked network structure with phase 5 and lamellar  $\text{Mg}(\text{OH})_2$ , thereby forming a high-strength solidification soil. The poor water resistance is due to the destruction of the network structure, resulting in the formation of loose triangular pyramid-shaped  $\text{Mg}(\text{OH})_2$  and  $\text{MgCO}_3$ .
- (5) In this paper, optimal raw material ratio range of MOC curing agent is given. Experiments and microscopic analysis are conducted to investigate the process that MOC enhanced soil. Subsequent experiments can be refined with reference to the given ratio range and mathematical model. Moreover, the test found that the water stability and water resistance of MOC solidified soil were poor. Follow-up research could focus on improving the water resistance of MOC solidified soil.

#### Data Availability

The data used to support the findings of this study are included within the article.

## Conflicts of Interest

The authors declare that they have no conflicts of interest.

## Acknowledgments

This study was supported by the Science and Technology Department Project of Qinghai Province (2021-QY-216) and Transportation Department Project of Qinghai Province (2019-14).

## References

- [1] Y. M. Zheng, H. Sun, M. X. Hou, and G. Xiurun, "Micro-structure Evolution of Soft clay under Consolidation Loading," *Engineering Geology*, vol. 293, Article ID 106284, 2021.
- [2] B. Apinun, H. Suksun, U. Artit et al., "Durability improvement of cement stabilized pavement base using natural rubber latex," *Transportation Geotechnics*, vol. 28, Article ID 100518, 2021.
- [3] S. Li, J. Yang, Y. Wu, and M. Wang, "Study on tensile properties of cement-solid soft soil," *Journal of Central South University*, vol. 53, no. 07, pp. 2619–2632, 2022.
- [4] S. Jahandari, M. Saberian, Z. Tao et al., "Effects of saturation degrees, freezing-thawing, and curing on geotechnical properties of lime and lime-cement concretes," *Cold Regions Science and Technology*, vol. 160, pp. 242–251, 2019.
- [5] M. Saberian, S. Jahandari, J. Li, and F. Zivari, "Effect of curing, capillary action, and groundwater level increment on geotechnical properties of lime concrete: experimental and prediction studies," *Journal of Rock Mechanics and Geotechnical Engineering*, vol. 9, no. 4, pp. 638–647, 2017.
- [6] F. D. S. J. Tennison, S. H. Karla, F. Silva Cezar, and R. Dalla, "Mechanical Behavior and Durability of a Typical Frictional Cohesive Soil from Rio Grande Do Sul/Brazil Improved with Portland cement," *Transportation Geotechnics*, vol. 34, 2022.
- [7] A. Pivák, M. Pavlíková, M. Záleská et al., "Foam glass lightened sored's cement composites doped with coal fly ash," *Materials*, vol. 14, no. 5, p. 1103, 2021.
- [8] A. Pham Tuan, K. Junichi, and D. Daniel, "Optimum Material Ratio for Improving the Performance of Cement-Mixed soils," *Transportation Geotechnics*, vol. 28, 2021.
- [9] J. F. Zhu, R. Q. Xu, Z. Y. Luo, B. Pan, and C. Rao, "Nonlinear constitutive model of magnesia cement-solidified soil considering the effect of curing agent dosage," *Rock and Soil Mechanics*, vol. 41, no. 7, pp. 2224–2232, 2020.
- [10] L. C. Yu, C. Yan, S. L. Guo, C. Yan, and X. Lin, "Effect of organic matter content on the properties of magnesium phosphate cement-solidified soil," *Chinese Journal of Engineering Geology*, vol. 28, no. 2, pp. 335–343, 2020.
- [11] R. Rintu, R. Dilan, S. Sujeeva, C. Susanga, and M. Abbas, "Optimization of fly ash based soil stabilization using secondary admixtures for sustainable road construction," *Journal of Cleaner Production*, vol. 294, Article ID 126264, 2021.
- [12] C. Hu, X. Z. Weng, C. Liu, L. Jiang, J. Liu, and W. Li, "Performance of polypropylene fiber-reinforced solidified soil," *Advances in Civil Engineering*, vol. 2021, Article ID 8859358, 16 pages, 2021.
- [13] T. Zhang, Y. L. Yang, and S. Y. Liu, "Application of biomass by-product lignin stabilized soils as sustainable Geomaterials: a review," *Science of the Total Environment*, vol. 728, Article ID 138830, 2020.
- [14] Ta Zhang, S. Y. Liu, H. B. Zhan, M. Chong, and C. Guojun, "Durability of silty soil stabilized with recycled lignin for sustainable engineering materials," *Journal of Cleaner Production*, vol. 248, no. C, Article ID 11293, 2020.
- [15] T. A. Aiken, M. Russell, D. McPolin, B. Gavin, L. Nugent, and L. Bagnall, "Effect of molar ratios and curing conditions on the moisture resistance of magnesium oxychloride cement," *Journal of Materials in Civil Engineering*, vol. 34, no. 2, 2022.
- [16] Q. Huang, W. X. Zheng, X. Y. Xiao, J. Dong, J. Wen, and C. Chang, "A study on the salt attack performance of magnesium oxychloride cement in different salt environments," *Construction and Building Materials*, vol. 320, Article ID 126224, 2022.
- [17] A. Maier and D. L. Manea, "Perspective of using magnesium oxychloride cement (MOC) and wood as a composite building material: a bibliometric literature review," *Materials*, vol. 15, no. 5, p. 1772, 2022.
- [18] A. Singh, R. Kumar, and P. Goel, "Factors influencing strength of magnesium oxychloride cement," *Construction and Building Materials*, vol. 303, Article ID 124571, 2021.
- [19] A. Pivák, M. Pavlíková, M. Záleská et al., "Low-Carbon composite based on MOC, silica sand and ground porcelain insulator waste," *Processes*, vol. 8, no. 7, p. 829, 2020.
- [20] K. Li, Y. S. Wang, X. Wang et al., "Superhydrophobic magnesium oxychloride cement based composites with integral stability and recyclability," *Cement and Concrete Composites*, vol. 118, Article ID 103973, 2021.
- [21] K. Gu, B. Chen, W. L. Bi, and Y. Guan, "Recycling of waste gypsum in preparation of magnesium oxychloride cement (MOC)," *Journal of Cleaner Production*, vol. 313, Article ID 127958, 2021.
- [22] A. Pivák, M. Pavlíková, M. Záleská, M. Lojka, O. Jankovsky, and Z. Pavlik, "Magnesium oxychloride cement composites with silica filler and coal fly ash admixture," *Materials*, vol. 13, no. 11, p. 2537, 2020.
- [23] Y. Y. Guo, Y. X. Zhang, K. Soe, R. Wuhner, W. D. Hutchison, and H. Timmers, "Development of magnesium oxychloride cement with enhanced water resistance by adding silica fume and hybrid fly ash-silica fume," *Journal of Cleaner Production*, vol. 313, Article ID 127682, 2021.
- [24] D. X. Wang, S. J. Di, X. Y. Gao, R. Wang, and Z. Chen, "Strength properties and associated mechanisms of magnesium oxychloride cement-solidified urban river sludge," *Construction and Building Materials*, vol. 250, Article ID 118933, 2020.
- [25] D. X. Wang, X. Y. Gao, X. Q. Liu, and G. Zeng, "Strength, durability and microstructure of granulated blast furnace slag-modified magnesium oxychloride cement solidified waste sludge," *Journal of Cleaner Production*, vol. 292, Article ID 126072, 2021.
- [26] D. X. Wang and Z. G. Chen, "Mechanical properties and microscopic mechanism of sludge solidified by magnesium oxychloride cement," *Geotechnical Mechanics*, vol. 42, no. 01, pp. 77–85+92, 2021.
- [27] F. T. Wang, K. Q. Li, and Y. Liu, "Optimal water-cement ratio of cement-stabilized soil," *Construction and Building Materials*, vol. 320, 2022.
- [28] J. Pooni, D. Robert, F. Giustozzi, S. Setunge, Y. M. Xie, and J. Xia, "Novel use of calcium sulfoaluminate (CSA) cement for treating problematic soils," *Construction and Building Materials*, vol. 260, 2020.
- [29] I. M. Power, G. M. Dipple, and P. S. Francis, "Assessing the carbon sequestration potential of magnesium oxychloride cement building materials," *Cement and Concrete Composites*, vol. 78, pp. 97–107, 2017.